Time Domain Simulation of Brass Instruments

Time Domain Simulation of Brass Instruments

Stefan Bilbao
Acoustics and Fluid Dynamics Group/Music
University of Edinburgh

Summary
Brass instrument modelling and synthesis poses many challenges, regardless of the type of numerical techniques employed; this is particularly true of the instrument bore, when boundary layer losses and nonlinear effects are included. Because the system is well modelled in 1D, finite difference time domain (FDTD) methods are a good match, and allow direct modelling for general instrument bores without the need for specialized filter structures, or calibration from measured impedance curves. The framework is well-suited for an extension to the case of fully nonlinear wave propagation, which is the ultimate goal of this work. In this paper, a simple FDTD scheme is applied to the brass instrument bore, in the context of sound synthesis, including viscous losses, and acoustic radiation. The extension to the case of fully nonlinear propagation is also discussed. Sound synthesis examples will be presented.

PACS no. 43.75.Fg

1. Introduction

Brass instrument physics, with the exception of the lip mechanism, is relatively well understood compared to that of most other instrument families, at least in the case of linear wave propagation in a single tube [1, 2]. Physical modeling sound synthesis methods (including digital waveguides [3]) are often based on a time-domain input/output formulation, which has its roots in the work of McIntyre et al. [4].

In the interest of exploring the extension to more realistic instrument configurations, involving time-varying tube networks (valves) and nonlinear wave propagation effects, it is useful to make use of finite difference time domain (FDTD) methods, which are very well suited to problems in one spatial dimension. "Time domain" here is meant in a different sense than that above, in that one also has a full spatial representation of the acoustic tube at hand. Such methods can be more computationally intensive than delay-line based methods, but such expense is not extreme by today's standards. The benefit is that there are fewer hypotheses made in the transition from a model system to a synthesis method, and thus a clearer link to the underlying physical model, which can be obscured when various assumptions (i.e., those that lead to efficient performance, such as propagation in delay lines, and lumping of various features, including distributed nonlinearity) are made.

A linear acoustic tube model, including radiation and viscothermal losses is presented in Section 2, and a standard FDTD scheme follows in Section 3. Simulation results are presented in Section 4. Some comments on an extension to the case of fully nonlinear acoustic wave propagation (important in high amplitude playing) are offered in Section 5. Though the lip mechanism is not described here, it is not difficult to couple such a scheme to a finite difference model; sound examples for such an instrument under playing conditions, generated in the Matlab environment, are available at

`http://www2.ph.ed.ac.uk/~sbilbao/brasspage.htm`

2. Acoustic Tube Models

2.1. Lossless Tubes

The following well-known pair of equations results from the linearization of conservation laws describing fluid flow in a 1D acoustic tube:

$$p_t + \frac{\rho c^2}{S}(Sv)_x = 0 \qquad v_t + \frac{1}{\rho}p_x = 0 \tag{1}$$

Here, $p(x,t)$ and $v(x,t)$ are the pressure deviation (from atmospheric) and particle velocity at coordinates $x \in [0, L]$ and $t \geq 0$ along a tube of length L m; ρ is the density of air, in kg/m^3 and c is the speed of sound, in m/s. Subscripts x and t indicate partial differentiation with respect to a spatial coordinate (of which there are various choices [5]) and time. $S(x)$ is the surface area of the tube at location x. See Figure 1. The first order system above will be retained

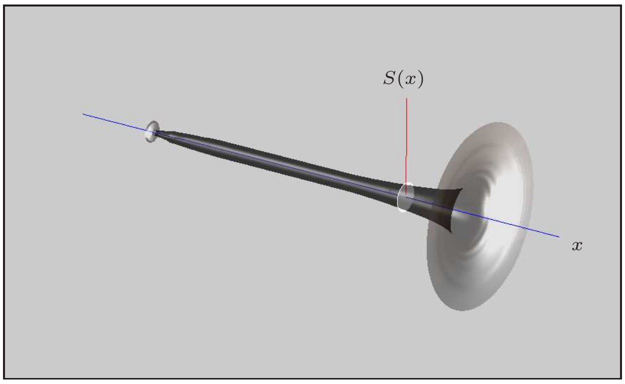

Figure 1. An acoustic tube, of cross-section $S(x)$.

here, rather than the second-order form (Webster's equation) which results from the combination of the two equations. It is useful to maintain the first order system, as it is a good to match to FDTD techniques, and, furthermore, allows the generalization to the case of nonlinear wave propagation. Such a system is a typical starting point for physical modeling sound synthesis for acoustic tubes, dating back as far as the well-known Kelly-Lochbaum model [6].

2.2. Bell Radiation

Bell radiation is typically framed in terms of an impedance, relating pressure and velocity. In general, it is not straightforward to employ such an impedance in an FDTD setting, unless it is of the form of a rational positive real function. The simplest possible such form (one pole, one zero, as is used often in speech synthesis [7]) leads to the following relationship between $v(x=L,t)$ and $p(x=L,t)$:

$$Z_c v = \alpha p + \beta m \qquad p = \frac{dm}{dt} \tag{2}$$

where $m = m(t)$ is an extra lumped variable, necessary here, as the boundary condition incorporates effects of inertia. The parameters α, β, and Z_c are defined by

$$\alpha_1 = \frac{1}{4(0.6133^2)} \quad \alpha_2 = \frac{c}{0.6133r} \quad Z_c = \rho c \tag{3}$$

where r is the radius of the bell opening.

This particular approximation matches rather well with more refined approximations used in brass instrument models [8]. Higher order rational approximations are a possibility [9], and as long as the corresponding impedance remains positive real, the FD procedure to be discussed below may be generalized without risk of instability.

2.3. Viscothermal Losses

Most models of viscothermal losses in acoustic tubes are based on a transmission line, or frequency domain formulation [10, 8]. As in the case of bell radiation, such forms may be converted into a time/space equivalent, which generalizes (1):

$$p_t + \frac{\rho c^2}{S}(Sv)_x + f p_{t^{\frac{1}{2}}} = 0 \tag{4a}$$

$$v_t + \frac{1}{\rho}p_x + g v_{t^{\frac{1}{2}}} = 0 \tag{4b}$$

Fractional derivative terms have appeared (as also appear in recent work on acoustic tube modeling in the scattering framework [11], employing the Webster-Lokshin equation, which is a second order form, simplified slightly from the above system). The new loss terms are spatially dependent:

$$f(x) = 2(\alpha-1)\sqrt{\frac{\eta\pi}{\nu\rho S(x)}} \quad g(x) = 2\sqrt{\frac{\eta\pi}{\rho S(x)}} \tag{5}$$

Here, α is the ratio of specific heats for air, and where ν and η are thermodynamic constants (see Keefe [10] for precise values). Higher order terms (which play a role only for very thin acoustic tubes) have been neglected here.

3. FDTD Schemes

3.1. Simple Scheme for the Lossless System

FDTD schemes were initially developed in order to time integrate the equations of electromagnetics [12, 13], usually employing interleaved grids, reflecting the symmetry between the dynamics of the electric and magnetic fields. The same symmetry holds in acoustics as well, and such interleaved schemes will be used here. The following scheme for system (1) is a generalization of FDTD to accommodate spatial variation:

$$p_l^n - p_l^{n-1} + \frac{\lambda Z_c}{\bar{S}_l}\left(S_{l+\frac{1}{2}}v_{l+\frac{1}{2}}^{n-\frac{1}{2}} - S_{l-\frac{1}{2}}v_{l-\frac{1}{2}}^{n-\frac{1}{2}}\right)=0 \tag{6a}$$

$$v_{l+\frac{1}{2}}^{n+\frac{1}{2}} - v_{l+\frac{1}{2}}^{n-\frac{1}{2}} + \frac{\lambda}{Z_c}\left(p_{l+1}^n - p_{l-1}^n\right)=0 \tag{6b}$$

p_l^n is an approximation to $p(x,t)$ at $x = lh$, and $t = nk$, for integer n and l and $v_{l+\frac{1}{2}}^{n+\frac{1}{2}}$ to $v(x,t)$ at $x = (l+\frac{1}{2})h$, and $t = (n+\frac{1}{2})k$, again for integer n and l. k is the time step, and h the grid spacing. See Figure 2. The two functions $S_{l+\frac{1}{2}}$ and $\bar{S}_l$ are in general not the same, but both approximate $S(x)$ in the limit of small grid spacing. The Courant number $\lambda = ck/h$, [14] is important in the analysis of numerical stability, as discussed below.

For a tube of length L, one may set $N = L/h$, so that p_l^n runs over $l = 0, \ldots, N$, and $v_{l+\frac{1}{2}}^{n+\frac{1}{2}}$ over $l = 0, \ldots, N-1$. The endpoint values p_0^n must be set by connection to the lip mechanism, and p_N^n through an approximation to the bell radiation condition.

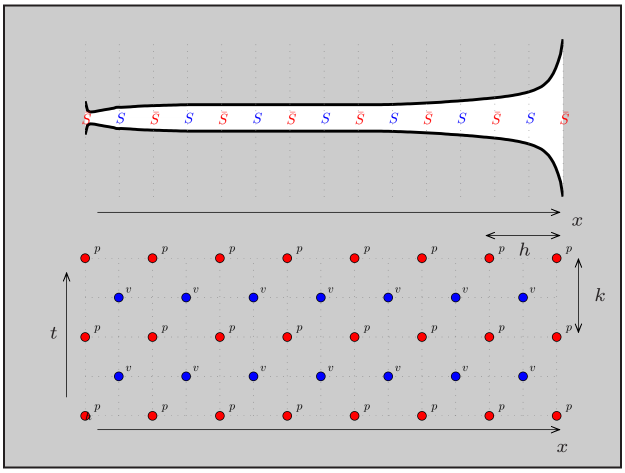

Figure 2. Profile of an acoustic tube, top, with approximations S and $\bar{S}$ at locations as indicated. Interleaved grid, bottom.

If $\bar{S}_l$ is chosen as $\bar{S}_l = (S_{l+\frac{1}{2}} + S_{l-\frac{1}{2}})/2$, then it is possible to show that the scheme is stable (over the interior)[15] if

$$\lambda \leq 1 \qquad \rightarrow \qquad h \geq ck \tag{7}$$

It should come as no surprise that the scheme can be rewritten in terms of wave variables, in a scattering context (the norm in sound synthesis applications). If $\lambda = 1$, the well-known Kelly Lochbaum model results [6], and for constant cross-section tubes, a bulk delay may be extracted to yield a standard digital waveguide formulation. The scheme above, however, is valid for $\lambda < 1$, which allows for some flexibility in the introduction of nonlinear terms. In general, however, a choice of λ near unity leads to a scheme with the least numerical dispersion, but also one of maximal computational complexity.

At the bell termination (right end), at grid location $l = N$, the update is

$$p_N^n - p_N^{n-1} + \frac{\lambda Z_c}{\bar{S}_l}\left(S_{N+\frac{1}{2}} v_{N+\frac{1}{2}}^{n-\frac{1}{2}} - S_{N-\frac{1}{2}} v_{N-\frac{1}{2}}^{n-\frac{1}{2}}\right) = 0 \tag{8}$$

which requires access to the virtual value $v_{N+\frac{1}{2}}$. An approximation to the radiation boundary condition (2), namely

$$v_{N+\frac{1}{2}}^{n-\frac{1}{2}} + v_{N-\frac{1}{2}}^{n-\frac{1}{2}} = \frac{\alpha_1}{Z_c}\left(p_N^n + p_N^{n-1}\right) + \frac{\alpha_2}{Z_c}\left(m^n + m^{n-1}\right) \tag{9}$$

$$p_N^n - p_N^{n-1} = \frac{k}{2}\left(m^n + m^{n-1}\right) \tag{10}$$

allows the closure of the system, where an extra update in a time series $m = m^n$ is required. The above boundary condition may be shown to be numerically passive [15], and thus there is no risk of numerical instability.

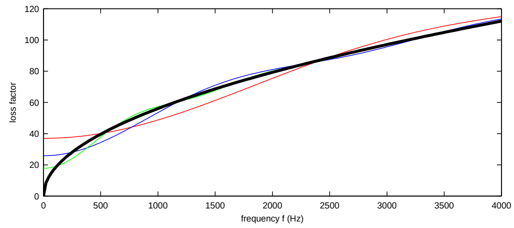

Figure 3. *Loss factor $\sqrt{\omega/2}$ as a function of ω, plotted as a thick black line, and approximations using 10th (red), 20th (blue) and 40th (green) order filters.*

3.2. Viscothermal Losses

The modeling of viscothermal losses is straightforward in the frequency domain; it is much more problematic in a time domain setting, due to the fractional derivative terms which appear in the model system. The obvious approach, and one used in the scattering context recently [11], is that of discrete-time approximation of the fractional derivative terms. For example, to approximate the term $p_{t^{\frac{1}{2}}}$ in (4a), one may employ the approximation

$$p_{t^{\frac{1}{2}}}(x,t) \approxeq \sum_{m=0}^{M} a_m p_l^{n-m} \tag{11}$$

for some parameters a_m, and for a chosen order M. Scheme (6) may thus be generalized to

$$p_l^n - p_l^{n-1} + \frac{\lambda Z_c}{\bar{S}_l}\left(S_{l+\frac{1}{2}} v_{l+\frac{1}{2}}^{n-\frac{1}{2}} - S_{l-\frac{1}{2}} v_{l-\frac{1}{2}}^{n-\frac{1}{2}}\right) + k f_l \sum_{m=0}^{M} a_m p_l^{n-m} = 0 \tag{12a}$$

$$v_{l+\frac{1}{2}}^{n+\frac{1}{2}} - v_{l+\frac{1}{2}}^{n-\frac{1}{2}} + \frac{\lambda}{Z_c}\left(p_{l+1}^n - p_{l-1}^n\right) + k g_{l+\frac{1}{2}} \sum_{m=0}^{M} a_m v_{l+\frac{1}{2}}^{n+\frac{1}{2}-m} = 0 \tag{12b}$$

where f_l and $g_{l+\frac{1}{2}}$ are approximations to $f(x)$ and $g(x)$ from (5) at locations $x = lh$ and $x = (l+\frac{1}{2})h$, respectively.

The determination of the parameters a_m may be accomplished by a variety of means; perhaps the simplest is to employ some form of optimization in the frequency domain (in which case the action of the operator $\partial_t^{\frac{1}{2}}$ may be viewed as multiplication by the factor $\sqrt{\omega}\mathrm{sign}(\omega)(1+j)/\sqrt{2}$, where ω is an angular frequency). It is the real part of this factor which gives rise to loss—the imaginary (reactive) part is insignificant compared to that of the lossless system, so it is probably sufficient to perform the optimization with respect to the real part only. See Figure 3, illustrating the approximation in the frequency domain for various orders M of approximation.

The order M of the approximation will determine the memory requirement for the algorithm as a whole, and has a strong impact on computational complexity. It would thus be advantageous to employ rational filter designs of potentially much lower order. Stability of the scheme (12), while unproven here (and rather difficult to show in general, for high order systems), has been observed under all conditions—loosely speaking, one may argue that any anomalous explosive behaviour at the Nyquist (the usual case) will be entirely dominated by the effects of loss due to bell radiation.

4. Simulation Results

4.1. Simulated Impedances

Simulated impedances for a variety of instrument bore profiles are presented in Figure 4. All have been generated using scheme (12) at 44.1 kHz, using a choice of λ as close to 1 as possible.

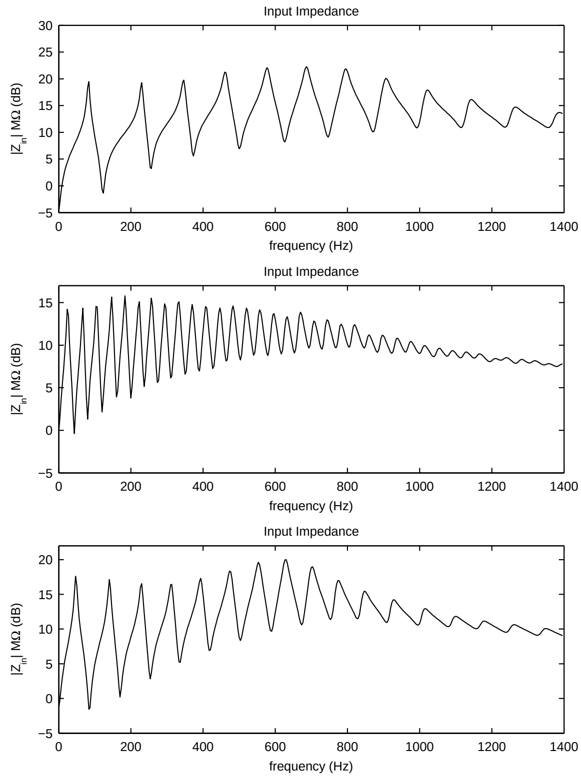

Figure 4. *Simulated input impedance magnitudes, for bore profiles corresponding to a trumpet (top), French horn (middle) and trombone (bottom).*

4.2. Accuracy

The basic scheme (6), in the absence of loss terms, is formally second-order accurate—the computed solution converges to the solution to (1) with error proportional to k^2 and h^2 (or either of the two quantities,

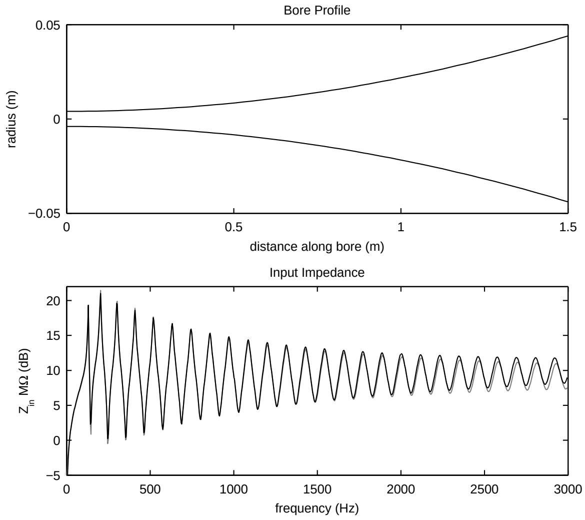

Figure 5. *A bore profile, top, and two input impedance curves, calculated at 96 kHz (black) and 16 kHz (grey).*

if k and h are related by a fixed choice of λ). In general, this order of accuracy is rather low—far more accurate choices for time discretization (such as, e.g., Runge Kutta methods [16]) and for spatial discretization (such as, e.g., pseudospectral methods [17]) are available.

In this particular case, however, formal accuracy analysis is somewhat misleading; for tubes of slowly varying cross-section, accuracy is excellent—this should come as no surprise, as in the case of a cylinder, and for $\lambda = 1$, the scheme computes an exact solution over the problem interior (and in fact can be reduced to a digital waveguide). The reason for this good behaviour can be seen in a more delicate analysis of the error terms in k and h, which in fact largely cancel, leading to good accuracy over the entire frequency range. See [15] for a complete analysis. (Indeed, if more formally accurate schemes are employed, though better accuracy is obtained at low frequencies, it can actually become worse at higher frequencies.)

As an example, consider input impedances calculated for a simple bore profile, at different sample rates, as illustrated in Figure 5; notice that the scheme produces comparable results for both high and low sample rates.

4.3. Sound Examples

Sound examples are available on the author's website at
`http://www2.ph.ed.ac.uk/~sbilbao/brasspage.htm`

5. Extensions to Nonlinear Wave Propagation

As should be clear from the introductory remarks, FDTD methods are by no means the only method (and certainly not the most efficient) available for simulating wave propagation in acoustic tubes. The time/space representation does have the advantage of allowing the introduction of more realistic features of wind instruments. Fully nonlinear propagation effects are among these, and may be expected to have important perceptual effects in instruments of long bore which are mainly cylindrical (such as the trombone [18]).

Returning to the lossless model of wave propagation in an acoustic tube given in (1), when nonlinear effects are introduced, the system is of the form

$$p_t + vp_x + \frac{\alpha}{S}\left(Sv\right)_x\left(p_0 + p\right) = 0 \tag{13a}$$

$$v_t + vv_x + \frac{1}{\rho}p_x = 0 \tag{13b}$$

where p_0 is the ambient pressure, and where ρ, is (a now variable) density. Such a system results from simplification of the Euler equations of fluid mechanics defined over a duct of variable cross-sectional area [19], under further assumptions of isentropic flow for polytropic gases (i.e., $(p + p_0) = \rho^{\alpha}$). Viscothermal effects are not included in the above model, and must be introduced with care, as such losses violate the underlying isentropic hypothesis. Further simplifications to this system, in particular for the case of cylindrical tubes, for which a decomposition into partially independent traveling wave components, have also been proposed for analysis of nonlinear wave propagation in brass instruments [20], and also in synthesis applications [21].

The main effect is that of shock formation, leading to increased brightness at high playing amplitudes. As the system above is of a form similar to the linear system (1), one should expect that FDTD methods (of which there are many varieties [22], including similar finite volume methods [23]) remain a viable solution method, and not of much greater computational expense (though stability analysis becomes formidable). See Figure 6, comparing the propagation of a sinusoidal input along a cylindrical tube under linear and nonlinear conditions. Easily visible is the progressive shock or N-wave formation, as well as numerical oscillations at the shock front.

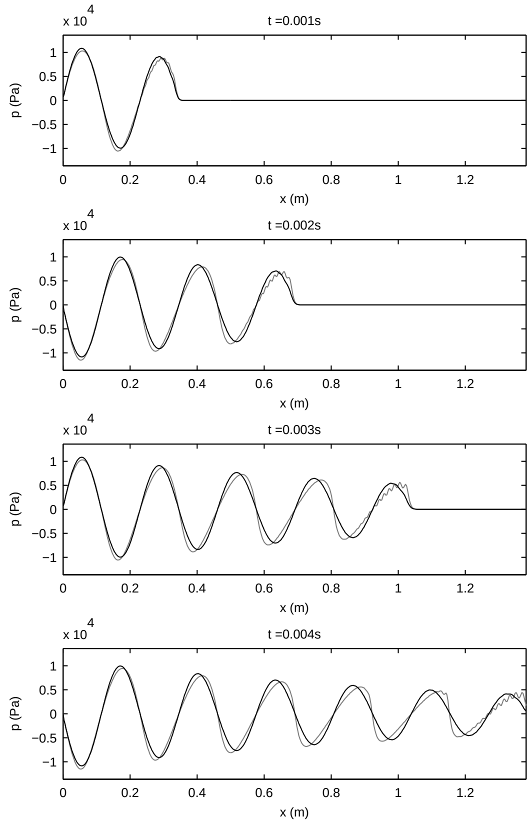

Figure 6. *Snapshots of wave propagation in a cylindrical tube under linear (black) and nonlinear (grey) conditions, at times as indicated.*

6. Conclusions and Future Work

The simulation method presented here is simple, and the basic intention here is not to develop of method which is extremely efficient, but rather one which is moderately efficient, simple to program, and capable of being generalized to handle more realistic features of wind instruments. In terms of programming simplicity, the great benefit is that there is no need to subdivide the bore into various segments (cylindrical, conical, etc.)—the bore is treated as a whole, including the mouthpiece and bell. As far as generalizability goes, many such features can be introduced, with a minimal effect on computational and programming complexity.

Among these are: 1) a lip model, which will require the solution of a separate set of ODEs at the left end of the tube, and to be coupled to the value p_0^n; 2) a more refined bell radiation model, which, provided that it is derived from a rational and positive real approximation to the radiation impedance, may be connected to the right end of the instrument with little difficulty, with some additional memory required in order to accommodate the reactive behaviour of the condition; 3) more refined one-parameter wave equations; 4) branched tubes and valves, under time-varying conditions, (though slides, requiring the introduction of time varying sections of tubing, and thus changes in total grid size, are much more problematic in the FDTD setting); and 5), nonlinear propagation effects, which, although they change little in the algorithm from the point of view of computational complexity, raise many additional concerns relating to numerical stability and aliasing. Features 1) and 4) are presently under study, and will be added to the present model in forthcoming work.

There are various weak points of the simulation method proposed here. One is the model of viscothermal loss, which is computationally costly, due to the use of FIR filter structures. It would be advisable to employ simple IIR structures, though it is anticipated that difficulties will arise when such schemes are used in a nonlinear setting. Another is, of course, numerical stability—while it is relatively straightforward to obtain stability conditions in the linear case, in the nonlinear case, this becomes much more difficult. It may be useful to reformulate the method in terms of the (very similar) finite volume methods, which rely directly on numerically conserved quantities. On the other hand, one of the usual difficulties with FDTD methods, namely numerical dispersion, does not figure strongly in this case, due to the particular nature of wave propagation in acoustic tubes.

Acknowledgement

Thanks to Shona Logie, John Chick and Arnold Myers, at the University of Edinburgh, for providing measurements of bore profiles and impedance curves for various brass instruments. Thanks to Joel Gilbert for comments on the nonlinear propagation aspect.

References

[1] A. Chaigne and J. Kergomard, *Acoustique des Instruments de Musique*, Belin, Paris, France, 2008.

[2] N. Fletcher and T. Rossing, *The Physics of Musical Instruments*, Springer-Verlag, New York, New York, 1991.

[3] J. O. Smith III, *Physical Audio Signal Procesing*, Stanford, CA, 2004, Draft version. Available online at `http://ccrma.stanford.edu/~jos/pasp04/`.

[4] M. McIntyre, R. Schumacher, and J. Woodhouse, "On the oscillations of musical instruments," *Journal of the Acoustical Society of America*, vol. 74, no. 5, pp. 1325–1345, 1983.

[5] T. Hélie, "Unidimensional models of acoustic propagation in axisymmetric waveguides," *Journal of the Acoustical Society of America*, vol. 114, no. 5, pp. 2633–2647, 2003.

[6] J. Kelly and C. Lochbaum, "Speech synthesis," in *Proceedings of the Fourth International Congress on Acoustics*, Copenhagen, Denmark, 1962, pp. 1–4, Paper G42.

[7] L. Rabiner and R. Schafer, *Digital Processing of Speech Signals*, Prentice-Hall, Englewood Cliffs, New Jersey, 1978.

[8] R. Caussé, J. Kergomard, and X. Lurton, "Input impedance of brass musical instruments—comparison between experiment and numerical models," *Journal of the Acoustical Society of America*, vol. 75, no. 1, pp. 241–254, 1984.

[9] F. Silva, P. Guillemain, J. Kergomard, B. Mallaroni, and A. Norris, "Approximation forms for the acoustic radiation impedance of a cylindrical pipe," *Journal of Sound and Vibration*, vol. 322, pp. 255–263, 2009.

[10] D. Keefe, "Acoustical wave propagation in cylindrical ducts: Transmission line parameter approximations for isothermal and nonisothermal boundary conditions," *Journal of the Acoustical Society of America*, vol. 75, no. 1, pp. 58–62, 1984.

[11] R. Mignot and T. Hélie, "Acoustic modelling of a convex pipe adapted for digital waveguide simulation," in *Proceedings of the 13th International Digital Audio Effects Conference*, Graz, Austria, September 2010.

[12] A. Taflove, *Computational Electrodynamics*, Artech House, Boston, Massachusetts, 1995.

[13] K. Yee, "Numerical solution of initial boundary value problems involving Maxwell's equations in isotropic media," *IEEE Transactions on Antennas and Propagation*, vol. 14, pp. 302–307, 1966.

[14] J. Strikwerda, *Finite Difference Schemes and Partial Differential Equations*, Wadsworth and Brooks/Cole Advanced Books and Software, Pacific Grove, California, 1989.

[15] S. Bilbao, *Numerical Sound Synthesis: Finite Difference Schemes and Simulation in Musical Acoustics*, John Wiley and Sons, Chichester, UK, 2009.

[16] F. Q. Hu, M. Y. Hussaini, and J. L. Manthey, "Low-dissipation and low-dispersion runge-kutta schemes for computational acoustics," *Journal of Computational Physics*, vol. 124, pp. 177–191, 1996.

[17] L. Trefethen, *Spectral Methods in Matlab*, SIAM, Philadelphia, Pennsylvania, USA, 2000.

[18] A. Hirschberg, J. Gilbert, R. Msallam, and A. Wijnands, "Shock waves in trombones," *Journal of the Acoustical Society of America*, vol. 99, no. 3, pp. 1754–1758, 1996.

[19] P. Roe, "Characteristic based schemes for the euler equations," *Ann. Rev. Fluid Mech.*, vol. 18, pp. 337–365, 1986.

[20] J. Gilbert, L. Menguy, and M. Campbell, "A simulation tool for brassiness studies," *Journal of the Acoustical Society of America*, vol. 123, no. 4, pp. 1854–1857, 2008.

[21] C. Vergez and X. Rodet, "A new algorithm for nonlinear propagation of sound wave: Application to a physical model of a trumpet," *Journal of Signal Processing*, vol. 4, pp. 79–88, 2000.

[22] G. Sod, "A survey of several finite difference methods for systems of nonlinear hyperbolic conservation laws," *Journal of Computational Physics*, vol. 27, no. 1, pp. 1–31, April 1978.

[23] R. Leveque, *Finite Volume Methods for Hyperbolic Problems*, Campbridge University Press, Cambridge, UK, 2002.